Eur. Phys. J. B **7**, 251–262 (1999)

THE EUROPEAN PHYSICAL JOURNAL B

EDP Sciences

New concepts for the slippage of an entangled polymer melt at a grafted solid interface

C. Gay[a]

Collège de France, Physique de la Matière Condensée[b], 11 place Marcelin Berthelot, 75231 Paris Cedex 05, France

Received: 20 February 1998 / Revised: 11 June 1998 / Accepted: 4 August 1998

Abstract. Molecular models of interfacial friction between an entangled melt and a compatible polymer brush (irreversibly grafted chains) are discussed. Progress since the 1992 model by Brochard and de Gennes is described, including the impact of the experimental evidence obtained by Durliat (thesis, 1997). A new, more realistic description of interfacial friction is adapted from the bulk tube renewal mechanism. It justifies some earlier results more precisely. It additionally predicts a progressive thinning of the grafted layer when the melt velocity exceeds some threshold value. An outline of the expected chain behaviour at very high grafting densities is given. It includes topological effects similar to combing.

PACS. 83.50.Lh Interfacial and free surface flows; slip – 83.20.Fk Reptation theories – 36.20.Ey Conformation (statistics and dynamics)

1 Introduction

In 1931, Mooney showed that slip may occur at the interface between a polymer melt and a solid wall [1]: the melt velocity V at the wall is nonzero, and the velocity profile extrapolates to zero beyond the solid wall. The corresponding distance b beyond the interface is known as the *extrapolation length*[1]. Such slip occurs when a very low mechanical coupling between the melt and the solid wall can be obtained. Conversely, the presence of anchored polymer chains at the interface increases friction significantly and thus reduces slippage. In such cases, the slip velocity is usually much too low to be observed, because the extrapolation length is much shorter than the characteristic sample thickness. But when the outflow is increased, a slip transition is observed as a pressure drop in capillary flows [3–7]: at low flow rates, the behaviour is compatible with a classical Poiseuille flow (*i.e.*, no observable slip), whereas at higher flow rates, a high slip velocity is infered from the pressure drop along the capillary, which is lower than that expected from a no-slip assumption.

This feature is important both from a fundamental point of view and because of its applications. Indeed, it is believed to have implications for extrusion processes: it might account for some of the instabilities that appear in the extrudate aspect at high imposed flow rates [4,8]. One explanation for the slip transition is that when anchored chains stretch at high fluid velocities, their interactions with the melt are reduced and slippage is enhanced. For extrusion, the anchored chains are adsorbed on the wall. In such a situation, the slip transition is sometimes caused not only by chain stretching, but also by chain debonding [7] under flow. In the present paper, we concentrate on situations (both experimental and theoretical) where no debonding takes place, and where it is thus possible to infer and to test some hypothesis on the dynamics of entangled flexible polymers.

In order to investigate the effect of interfacial chains in a controled manner, Durliat, Folkers, Hervet, Léger, Massey and Migler led carefully designed experiments [9–14]. Couette flow was chosen for the shear stress to be uniform: no shear-dependent bulk phenomenon should occur at the interface specifically because of the non-uniform shear stress, as it could in capillary experiments with Poiseuille flow. The experimental set-up makes it possible to detect and to measure not only the high slip velocities, but also the low slippage velocities V that occur before the slip transition. Surface treatment is essential for the control of the presence and number of polymer chains at the interface; the theoretical interpretation is made easier because it is possible to use grafted, reasonably monodisperse chains (N monomers) rather than adsorbed layers. Melts of different degrees of polymerization (P monomers per chain) are used.

The typical observed variations of $b(V)$ are shown in Figure 1a. A low slip regime ($b = b_0 \approx 1$ to 3 μm) is

[a] e-mail: cgay@pobox.com

Present address: Laboratoire CNRS-Elf Atochem (UMR 167), 95 rue Danton, B.P. 108, 92303 Levallois-Perret Cedex, France.

[b] URA 792 du CNRS

[1] The explanation for the existence of slip is as follows [2]. The friction between the solid wall and each monomer that is in contact with it is independent of the melt chain length. On the opposite, the melt viscosity strongly depends on the melt molecular weight. Hence, very high values of the extrapolation length can be obtained for long chains.

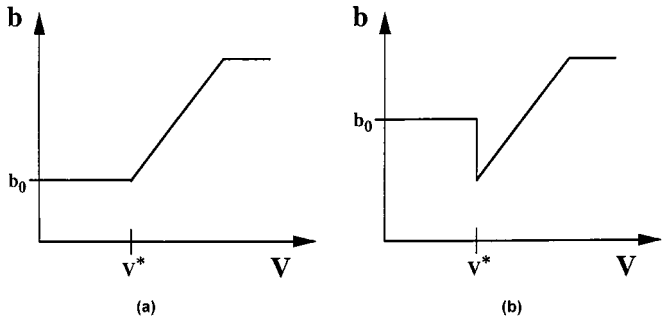

Fig. 1. Extrapolation length b as a function of the melt velocity V at the interface: low slip plateau at small velocity, marginal regime with $b \propto V$, high slip plateau at high velocities. (a) Typical aspect of the experimental curves. (b) Predictions of the 1992 model: the drop of $b(V)$ at $V = V^\star$ is not observed experimentally.

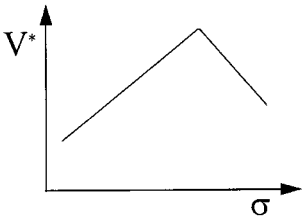

Fig. 2. Dependence of the threshold velocity $V^\star$ on the grafting density σ, as obtained experimentally by Durliat (schematic outline).

present at low velocities ($V < V^\star \approx 10$ μm/s) and a high slip regime ($b = b_\infty \approx 30$ to 100 μm) occurs at high velocities ($V > V_\infty \approx 100$ μm/s). In the intermediate regime ($V^\star < V < V_\infty$), the extrapolation length b increases linearly with velocity[2]. Recent work by Durliat [14] made it possible to control the grafting density σ. The corresponding variation of the critical velocity $V^\star(\sigma)$ could be obtained (Fig. 2).

Since the observed extrapolation lengths b are much greater than the chain dimensions (radii of gyration of at most 50 nm), the velocity field can be considered as uniform on the molecular scale. Therefore, we need to model the interactions between grafted chains and a melt moving at velocity V. The 1992 model built by Brochard and de Gennes [15] accounts for most features of the experimental results available at the time. It correctly predicts the low slip regime at low velocities, the marginal regime ($b \propto V$) at intermediate velocities ($V^\star \leq V \leq V_\infty$) and the high slip at high velocities. It also predicts the correct dependence of $V^\star$ on the melt molecular weight P.

It additionally predicts, however, a sharp drop of the extrapolation length $b(V)$ just before the marginal regime, for $V \simeq V^\star$ (Fig. 1b). No such drop was observed, and attempts were made to modify the model in order to eliminate this aspect of the predictions.

In the present paper, we summarize the improvements that were brought to the 1992 model [16–20]: most experimental results can be explained, which allows for much confidence in the modified model, even though there remains a strong discrepancy in the absolute orders of magnitude. We also present a new approach of the friction mechanism [21] and we outline a topologically driven behaviour (combing effect) at very high grafting densities.

2 The 1992 model

We here present the main elements of the 1992 model, in order to determine in which way it can be modified.

In the 1992 model, the description of friction is based on the *forced sliding mechanism* [22,15][3]. The conformations of the grafted N chains can be considered as frozen, because their relaxation is similar to that of branched polymers, *i.e.*, very slow [24]. Hence, mobile chains P that get into close contact with an N chain have to slide quickly around the grafted obstacle since their Edwards' tube is being pinched by the fixed N obstacle. The allowed sliding time t_s is fixed by the pinching time, which is typically the tube diameter divided by the velocity ($t_s = aN_e^{1/2}/V$). The resulting curvilinear, sliding velocity $V_{tube} = L_{tube}/t_s$ (where $L_{tube} = (P/N_e)\Lambda_e$ is the tube length) is much faster than the overall melt velocity V:

$$V_{tube} = \frac{P}{N_e} V. \tag{1}$$

Consequently, the additional dissipation $T\dot{S} \simeq P\zeta_0 V_{tube}^2$ caused by each sliding P chain corresponds to the work of a force

$$f \simeq \frac{P^3}{N_e^2}\zeta_0 V \simeq a\eta_P^{rep} V \tag{2}$$

exerted by each P chain that is entangled with a grafted chain, where η_P^{rep} is the expression of the melt viscosity as derived from the reptation models [25,23].

The total force F exerted on a grafted chain depends on the average number X of P chains entangled with each grafted chain:

$$F = X\, f. \tag{3}$$

In the 1992 model, the *trapping number* X is derived from the *total entanglement* assumption: all P chains are supposed to be trapped if they intersect the volume pervaded by the grafted N chain. Hence (taking $P \geq N$, which is the experimental situation), it reads:

$$X_{tot} = N^{1/2}. \tag{4}$$

[2] In the case of adsorbed chains, the dependence of the extrapolation length on the velocity is usually non-linear: $b \propto V^\alpha$, with $\alpha = 0.5$ to 1 [14]. We here only consider brushes. The observed exponent α is then equal to unity.

[3] A similar mechanism was introduced by de Gennes to give a direct derivation of the viscosity of an entangled melt [23].

If the force F is weak enough ($F \leq kT/(aN^{1/2})$), the grafted chain does not deform. Consequently, the trapping number is constant and friction is proportional to velocity: $F = Xf \propto V$. If σ/a^2 is the number of grafted chains per unit area, this corresponds to a constant extrapolation length

$$b = \frac{a^2\eta_P V}{\sigma F} = \frac{a}{\sigma N^{1/2}}\frac{\eta_P}{\eta_P^{rep}} \equiv b_0, \tag{5}$$

valid at velocities smaller than some value V_0 given by $F \simeq kT/(aN^{1/2})$, *i.e.*, $N^{1/2}a\eta_P^{rep}V_0 \simeq kT/(aN^{1/2})$.

At higher velocities, the chain is deformed and the trapping number is modified. Indeed, the chain is turned into a string of blobs of size Λ given by $F \simeq kT/\Lambda$ (Pincus' relation [26]). The corresponding trapping number $X = (N/g)X(g)$ (where g is the number of monomers per blob, with $\Lambda = ag^{1/2}$) is greater than the initial value $X(N)$ given by equation (4). As a result, the chain is stretched even further and friction is enhanced, in a self-consistent manner. This feature causes b to decrease with increasing V in this regime $V > V_0$, instead of being independent of velocity. Because the exponent value is 1/2 in equation (4), the decrease of $b(V)$ is a sharp drop, as was described above (Fig. 1b). Indeed, we have simultaneously $X = (N/g)g^{1/2}$ and $F = Xf = kT/(ag^{1/2})$, which implies $V = V_0$ for all g.

When the blob size Λ reaches the entanglement tube diameter $\Lambda_e \simeq aN_e^{1/2}$, it has decreased by a factor $(N/N_e)^{1/2}$. The force is then given by $F \simeq kT/\Lambda_e$, and the extrapolation length $b = (a^2\eta_P V_0/(\sigma F) = (N_e/N)^{1/2}b_0$ (when V just exceeds V_0) is much lower[4] than for lower velocities $V < V_0$. This marks the onset of the *marginal regime* [15] ($V \geq V^\star$, with $V^\star \approx V_0$ in the present case), in which the force F remains constant over a whole range of melt velocities. Indeed, if the blob size were to decrease any further, complete disentanglement would take place, friction would be significantly lowered and the blobs would swell again. If, on the opposite, the blob size were larger than Λ_e, the exerted force would stretch the chain beyond Λ_e. Hence, elongation is constant ($\Lambda \simeq \Lambda_e$) and consequently, the force is constant[5]:

$$F^\star \simeq kT/\Lambda_e \tag{6}$$

and the extrapolation length is proportional to velocity: $b \propto V/F^\star \propto V$.

[4] Experimentally, the velocity V_0 is reached progressively and there should be a transition between $b = b_0$ and the lower value of b. Here, we only describe the permanent regime, where $b = (N_e/N)^{1/2}b_0$ as soon as V just exceeds V_0.

[5] Another, more realistic interpretation [16,17] of the marginal regime is that the main part of the chain ("stem") is elongated just beyond Λ_e. The stem is subjected to a weak friction from the melt (disentangled regime) but it is stretched by the tension that is transmitted from the stronger friction on the "flower" (weakly stretched chain free end). The size of the flower naturally adjusts so that the remaining stem only feel the disentangled friction (*i.e.*, $\Lambda \simeq \Lambda_e$), since the flower precisely consists in the part of the chain which is less deformed ($\Lambda > \Lambda_e$).

Along with the entangled friction just described, there remains a disentangled, Rouse friction acting on every monomer: $F_{Rouse} = N\zeta_0 V$. In the marginal regime, the entangled component of friction is constant ($F \simeq F^\star = kT/\Lambda_e$). Hence [15], the Rouse friction becomes dominant at high velocities $V \geq V_{Rouse}$:

$$V_{Rouse} \simeq \frac{1}{NN_e^{1/2}}\frac{kT}{a\zeta_0} \tag{7}$$

$$F \simeq N\zeta_0 V. \tag{8}$$

The corresponding extrapolation length is constant and the origin of the final plateau $b = b_\infty$ is thus explained.

The predictions of the 1992 model account well for the main features of the experimental behaviour of the grafted surface. There remains the undesired prediction of a drop of $b(V)$, however. In an attempt to improve this point, each of the main elements of the model can be modified. In the following sections, we study successively the changes that can be brought by altering the friction mechanism, the trapping number, or by including collective effects of the grafted chains when the grafting density is increased.

3 Changing the friction mechanism

The sliding mechanism described for the P chains is in fact unrealistic at low velocities. Indeed, the reptation time $T_{rep}(P)$ of the P chains is shorter than the sliding time t_s, for all velocities $V < V^{\star\star}$ considered so far, where:

$$V^{\star\star} = \frac{\Lambda_e}{T_{rep}(P)}\,. \tag{9}$$

Hence, P chains spontaneously slide out from the N obstacle long before they could be forced to do so[6].

The forced sliding mechanism is not adequate to describe chain motion at high velocities either. Indeed, above $V^{\star\star}$, the forced sliding time t_s is shorter than the reptation time of P chains. As a result, if one P chain is forced to slide, it creates a net volume transfer near its end at too high a rate for relaxation to occur by mere reptation of the surrounding chains: distortion of the melt is likely to occur. Hence, the mechanism would have to be modified to include such distortions.

In the following paragraphs, we consider another friction mechanism which probably describes the chain motion more closely and which yields a consistent picture of both the low velocity regime ($V < V^{\star\star}$) and the high velocity regime ($V > V^{\star\star}$).

[6] The evaluation of the extra dissipation due to entanglements between P chains and N chains remains valid, however. But it must be considered as an average, slow drift, added to the diffusive reptation of P chains. Furthermore, the force f, as worked out therefrom (Eq. (2)), has no more significance as such, since each P chain does not dissipate during the entire time t_s. For the same reason, the work of the friction that is exerted on each P chain is insufficient to deform it: in all the models reviewed in this paper, whenever relevant, the melt chains are supposed to be Gaussian.

Tube renewal

The forced sliding mechanism is based on the consideration of the Edwards' tube of a P chain, which is squeezed by the N chain. Conversely, we here consider the tube of the N chain. It is made of short strands of the surrounding melt chains which locally act on the grafted chain as topological constraints. These P chains themselves are continually diffusing by reptation. Hence, the tube of the grafted N chain is progressively renewed as P chains diffuse away and are replaced with other chains. Since the conformations of new chains are never identical to those of previous chains, the tube of the N chain fluctuates. At low velocities, such fluctuations are equivalent to a friction force (fluctuation-dissipation theorem)[7].

This concept of *tube renewal* was introduced by Klein [27] and by Daoud and de Gennes [28] for the diffusion of a long N chain in a melt of shorter P chains: if the test chain is long enough, its own reptation among the P chains is a slower diffusion process than this tube renewal mechanism. We here adapt this concept to the case of a grafted chain [21]: since the usual reptational motion of the N chain is blocked due to grafting, tube renewal constitutes the dominant relaxation process, even in the case of longer surrounding chains[8].

Let us consider one particular entanglement blob of size Λ_e along the N chain. Many "quick" P chains enter the blob and then go out in the reverse direction after a short time. They induce small fluctuations of the N chain in the blob. But "slow" chains remain for a longer time: once the first end has entered the blob and after some diffusion back and forth, such a slow P chain usually quits the blob when the other end goes out, following the first. Slow chains remain present in the blob during about a reptation time $T_{rep}(P)$ and exert topological constraints. Hence, the characteristic time scale for tube renewal is the reptation time. The corresponding characteristic distance for blob fluctuations is of the order of the blob size $\Lambda_e = aN_e^{1/2}$. Therefore, the diffusion constant of the blob[9] is given by:

$$D(N_e) = \frac{(aN_e^{1/2})^2}{T_{rep}(P)} \frac{1}{k}, \tag{10}$$

where the constant k is to be chosen so as to obtain the correct order of magnitude for the fluctuations[10]. The diffusion of the whole N chain is thus characterized by:

$$D(N) = \frac{N_e}{N} \frac{(aN_e^{1/2})^2}{T_{rep}(P)} \frac{1}{K} \tag{11}$$

where the coefficient K includes both the constant k and possible correlations between the diffusion motions of different blobs along the chain. The corresponding friction coefficient for the chain in the melt at small velocities is deduced from the fluctuation-dissipation theorem and the friction force reads:

$$F = K\zeta_0 \frac{NP^3}{N_e^3} V. \tag{12}$$

Chain conformation and friction at high velocities

The threshold $V^{\star\star}$ (Eq. (9)) occurs within the marginal regime ($V^\star < V^{\star\star} < V_{Rouse}$): grafted chains are elongated, with $\Lambda = \Lambda_e$. The forced sliding mechanism (reinterpreted as an average drift) is suitable for describing the marginal regime at low velocities ($V^\star < V < V^{\star\star}$). But the tube renewal approach gives a new insight into the nature of the marginal regime and into chain behaviour at higher velocities.

In the marginal regime, the whole "stem" (upstream part of the chain) is supposed to be a string of blobs of size Λ_e or slightly smaller. Since the chain is significantly oriented on the Λ_e length scale, fluctuations due to the melt chains take place mainly in the directions perpendicular to stretching. Correlatively, friction in the direction of stretching (direction of flow) is weak in the stem. Only the downstream part of the chain ("flower") is subjected to significant friction.

Above $V = V^{\star\star}$, the grafted chain is progressively flushed against the wall, *i.e.*, its lateral fluctuations are progressively reduced (Fig. 3). This transition can be understood very precisely in the tube renewal approach. In the direction of flow, the interval Δx between consecutive blobs is always of the order of Λ_e (Fig. 4a). In the perpendicular directions, the distance Δy between consecutive blobs depends both on diffusion (characterized by Eq. (10)) which tends to increase the interval (Fig. 4b), and on the chain tension $F^\star \simeq kT/\Lambda_e$ which tends to reduce it (Fig. 4c).

Below $V^{\star\star}$, the diffusion process is strong enough for tension to play a role. The chain tension $F^\star$ gives rise

[7] This tube renewal mechanism is thus another way of describing the friction due to entanglements between grafted and melt chains. In both cases, however, relaxation of the entanglements are due to the motion of the melt chains which is quicker than that of the grafted chains ("branched" reptation, see Ref. [24]).

[8] Rearrangement of the grafted chain takes over for ultralong melt chains, in the network limit.

[9] At a given time, a given strand of N_e monomers (of size roughly Λ_e) has a definite orientation: its end-to-end vector is either along the flow, or perpendicular to the flow, or in any intermediate direction. The diffusion constant given by equation (10) in fact describes the fluctuations of such a strand perpendicularly to its orientation. For instance, if it is oriented along the flow, it will describe its fluctuations perpendicularly to the flow. As long as the chain is not completely stretched ($V < V^\star$ and thus $\Lambda < \Lambda_e$), the orientation of such strands of N_e monomers are essentially random (the effect of stretching on orientation is then dominant only for long strands which have at least $g_\Lambda = \Lambda^2/a^2$ monomers). Hence, as long as $V < V^\star$, equation (10) describes the diffusion in all directions alike. In particular, it can be used to estimate the friction in the direction of flow.

[10] The value of k will be fixed later on (see Sect. 7).

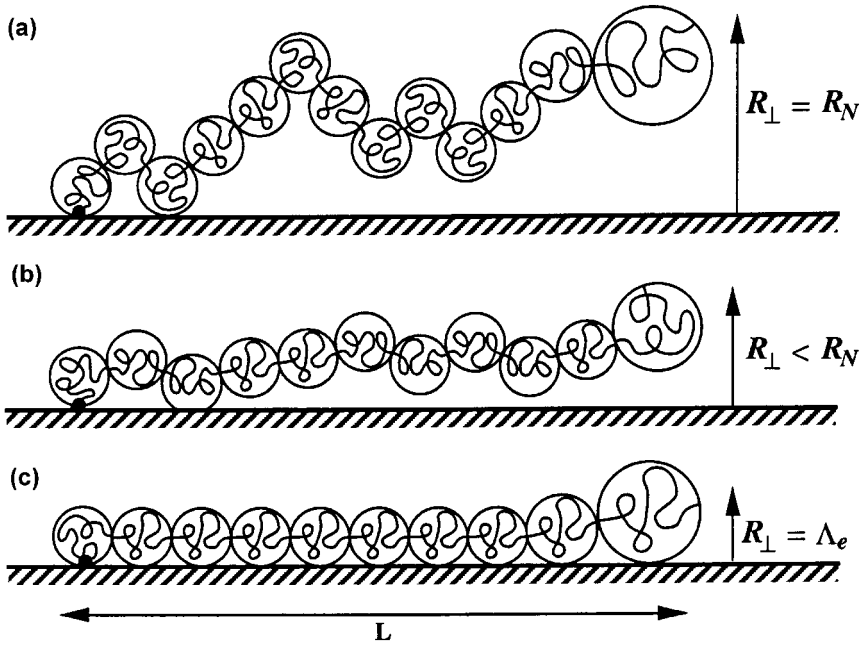

Fig. 3. Aspect of a grafted chain in the marginal regime. The blob size is of order Λ_e and the chain length is of order $\Lambda_e N/N_e$. The lateral fluctuations of the chain depend on velocity. (a) When $V < V^{\star\star}$, the transverse radius of gyration of the chain is unchanged: $R_\perp \simeq aN^{1/2}$. (b) At intermediate velocities $V^{\star\star} < V < V^{\star\star\star}$, the lateral fluctuations are reduced: $R_\perp \propto V^{-1/2}$. (c) When $V > V^{\star\star\star}$, the chain is completely flushed against the wall and the transverse radius of gyration is close to the blob size: $R_\perp \simeq \Lambda_e$.

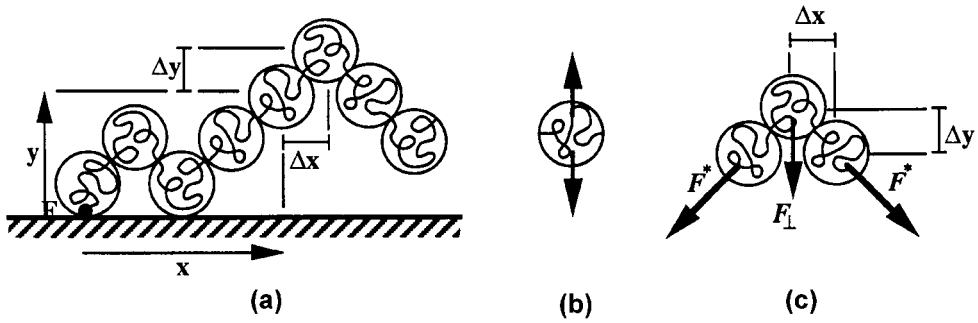

Fig. 4. Conformation of a grafted chain in the marginal regime. (a) In the direction of stretching, the interval between successive blobs is $\Delta x \simeq \Lambda_e$; in the perpendicular direction, the blobs form a random walk of unit steplength Δy. (b) The reptation of neighbouring chains makes the blobs fluctuate perpendicularly to the direction of stretching. (c) Due to the tension $F^* \simeq kT/\Lambda_e$ of the chain, the transverse interval Δy between blobs is drawn back by a force $F_\perp$.

to a pull-back force $F_\perp \simeq (\Delta y/\Delta x)F^\star$ which tends to align consecutive blobs. Deviations from the mean position $\Delta y = 0$ correspond to an elastic energy of order $F_\perp \Delta y$. The diffusion-driven, thermal exploration Δy is such that $F_\perp \Delta y \simeq kT$. Taking $\Delta x = \Lambda_e$ and $F^\star = kT/\Lambda_e$, this yields $\Delta y \simeq \Lambda_e$: this is the marginal regime as described earlier, with unperturbed transverse radius of gyration $R_\perp \simeq \Delta y(N/N_e)^{1/2} = aN^{1/2}$ (Fig. 3a).

Above $V^{\star\star}$, the chain tension plays no role because diffusion is slower and provides the upper bound for the chain fluctuations: the diffusion time L/V (where $L \simeq (N/N_e)\Lambda_e$ is the length of the stretched chain conformation) corresponds to lateral fluctuations of order:

$$R_\perp = \left[D(N_e)\frac{L}{V}\right]^{1/2} = aN^{1/2}\left[\frac{V^{\star\star}}{V}\right]^{1/2} \qquad (13)$$

and the chain conformation corresponds to Figure 3b.

At a higher velocity $V^{\star\star\star} = (N/N_e)V^{\star\star}$, the fluctuations are so slow that the stem of the chain is now straight (it is a "trunk" with $R_\perp \simeq \Lambda_e$, see Fig. 3c). Using neutron reflectivity, it might be possible to test whether the grafted chains are indeed flushed against the solid wall progressively from $R_\perp \simeq R_N$ to $R_\perp \simeq \Lambda_e$.

The friction is still of the marginal type (constant $F^\star = kT/\Lambda_e$) in these regimes, since the stem-flower description remains valid. Only at higher velocities does the Rouse (non-entangled) friction $F_{Rouse} = n\zeta_0 V$ on the trunk become dominant: as a consequence, above V_{Rouse}, the chain starts to elongate further, until it is completely stretched ($L \simeq Na$) above $V = V_3 = kT/(aN\zeta_0)$. Complete stretching has no significant influence on friction, however. Hence, no change should be observable macroscopically at V_3.

Formal equivalence with forced sliding mechanism

Comparing equations (2, 3) with equation (12), we see that the forced sliding and the tube renewal mechanisms

are formally equivalent if we set:

$$X \equiv K\frac{N}{N_e}\cdot \tag{14}$$

Hence, the expression for friction remains unchanged and no better predictions can be drawn from the tube renewal mechanism as compared to those of the 1992 forced sliding mechanism. It must be pointed out, however, that the tube renewal mechanism is far more realistic (see discussion after Eq. (9)) and brings a deeper understanding of the chain behaviour. These points are developed in Section 6.

4 Changing the trapping number

It was just shown in Section 3 that improving the elementary friction mechanism of the 1992 model is not sufficient to modify the predictions for the extrapolation length $b(V)$ (see Eq. (14)). In the present section, we investigate the improvements that can be brought by a modification of the trapping number X (Eq. (3)), which is the average number of melt chains P that are entangled with each grafted chain N.

The models

In the 1992 model, the trapping number is derived from the *total entanglement* assumption: any P chain that is present in the volume occupied by the grafted chain is subjected to entanglements from the grafted chain[11]. When $P \geq N$, the trapping number is thus given by equation (4). The local version of the total entanglement assumption corresponds to one possible description of an entanglement: in each entanglement blob Λ_e along the grafted chain N, *all* $N_e^{1/2}$ melt chain strands that are present *do participate* in the entanglement with the grafted chain.

Alternative descriptions have been suggested. The *binary entanglement model* [18] stipulates that in each entanglement blob, the grafted chain interacts only with *one other* chain. For the whole chain, this means that it is usually entangled with only N/N_e melt chains. Very long chains, however ($N > N^\star = N_e^2$), do trap all chains present (since the total number of melt chains, $N^{1/2}$, is then smaller than the number of available entanglements, N/N_e). But the corresponding threshold molecular weight ($N^\star$) is well beyond reach for current polymers[12]. The trapping number predicted by the binary entanglement model is thus given by the number of entanglements along the grafted chain:

$$X_{bin} = \frac{N}{N_e} \qquad (P \geq N). \tag{15}$$

The *correlated binary entanglement model* was introduced by Brochard, Ajdari, Leibler, Rubinstein and Viovy [17]. Entanglements are still supposed to be binary interactions (only two chains participate). But correlations are introduced: consider the grafted chain and a particular melt chain which is entangled with it. These two chains have a certain number x of entanglement blobs Λ_e in common. The interaction due to this melt chain is supposed to be lessened by the factor x. On the whole, the trapping number is thus supposed to be $X = (N/N_e)/x$ in the correlated binary entanglement model[13]:

$$X_{cor.bin.} = \frac{N^{1/2}}{N_e^{1/2}} \qquad (P \geq N). \tag{16}$$

Given the expression of the trapping number in the long melt chain limit ($P \geq N$), its value in the reverse situation $P \leq N$ is obtained by decomposing the longer N chain into sub-chains of P monomers:

$$X_{P\leq N} = \frac{N}{P}\,\left[X(N)|_{N=P}\right] \tag{17}$$

where $X(N)$ is given by equations (4, 15 or 16).

Predictions

Comparison of equations (4, 16) shows that the trapping number X is proportional to $N^{1/2}$ both in the total entanglement model and in the correlated binary entanglement model. Hence, both models yield the same qualitative results. In particular, sudden elongation of the grafted chains occurs from the coil conformation to the marginal regime conformation (see Sect. 2). This corresponds to the sharp drop of the extrapolation length $b(V)$, which was described earlier as the main mismatch with experimental observations. Hence, the correlated binary entanglement model does not seem to bring any improvement on this point[14].

Equation (15) shows that in the binary entanglement model, the trapping number is proportional to N. As a consequence, adapting the argument of Section 2, we find that the trapping number of the elongated chain, $X = (N/g)X(g)$ (where g is the number of monomers

[11] In the present discussion, we suppose that melt chains are longer than grafted chains ($P \geq N$). The values of the trapping number in the reverse situation can be deduced immediately, see equation (17).

[12] In reference [20], the real value of the threshold molecular weight is computed using tabulated data on some common polymer melts. The results should make it possible to compare the threshold values for different polymers (if such a threshold does exist). There remains a general, undetermined, multiplicative constant, however, since numerical factors are omitted in the whole study.

[13] Whatever the validity of expression (16) itself, the justification for it [17] seems inconsistent as such. Indeed, the quantity N/N_e is based on the binary assumption and means *one* interaction per entanglement blob (out of $N_e^{1/2}$ chain strands that are present within a blob), whereas x corresponds to one correlation for *each* common blob.

[14] Many-chain effects, however, erase this discrepancy, as will be shown in Section 5.

per blob) is *equal* to the initial value $X(N)$ given by equation (15). Hence, elongation occurs progressively with no change in the trapping number. Friction is still proportional to velocity and the extrapolation length displays no decrease [18] before it reaches the marginal regime.

Hence, the predictions of the binary entanglement model are better than those of the original, total entanglement model. They qualitatively match the experimental results for the extrapolation length[15]. Hence, this is one way of correcting the predictions.

5 Influence of the grafting density

The 1992 model is essentially a one-chain model. Although it was shown in Section 4 that a proper choice for the expression of the trapping number was one way of obtaining qualitatively correct predictions as for the extrapolation length, the modifications presented in Sections 3 and 4 do not incorporate any many-chain feature. In the present section, we describe how the effect of the grafting density can be taken into account [19].

As the grafting density is increased, the number σ_P of trapped melt chains per unit area of the solid surface also increases:

$$\sigma_P = \sigma\, X. \tag{18}$$

But there exists a geometrical limitation: all trapped P chains have to be located within reaching distance from the surface. If we restrict to $P \geq N$, the centers of gravity of the P chains have to be located within a distance of order R_P from the surface so that the chains do reach the grafted layer. Hence, the maximum chain trapping is given by:

$$\sigma_{Pmax} = a^2\, \frac{R_P}{Pa^3} = P^{-1/2}. \tag{19}$$

This maximum overall trapping is reached when the grafting density is greater than $\sigma^\star$ defined by:

$$\sigma^\star \equiv \frac{1}{P^{1/2}\, X} \tag{20}$$

where the explicit expression depends on the model for X (see Sect. 4). The change at $\sigma \simeq \sigma^\star$ is due to the onset of interference between the grafted chains: above $\sigma \simeq \sigma^\star$, although each melt chain can be trapped simultaneously by several grafted chains, it still must be counted as only one chain that is forced to slide out[16].

Predictions

Beyond $\sigma^\star$, the overall trapping is fixed at $\sigma_P = \sigma_{Pmax}$. Hence, the macroscopic surface behaviour is not sensitive to grafting any more. It does not depend on the model for the trapping number X either. In other words, the effect of grafting has *saturated*. At low velocities, the extrapolation length b is given by:

$$b_0 \simeq \frac{a}{\sigma_{Pmax}} \simeq aP^{1/2} = R_P. \tag{21}$$

At higher velocities, grafted chains start to elongate. As was pointed out in Section 4, elongation can only enhance the trapping efficiency of each grafted chain[17]. Hence, in the *saturated grafting* regime, elongation can only *reinforce* saturation. Correlatively, the overall amount of trapped chains remains fixed at $\sigma_P = \sigma_{Pmax}$ and the friction stress remains proportional to velocity even when chains are elongated:

$$\tau = \sigma_{Pmax}\, f \qquad (\sigma \geq \sigma^\star,\, V \leq V^\star) \tag{22}$$

where f is given by equation (2). The extrapolation length is thus constant and equal to b_0 (Eq. (21)). The velocity V_0 at which grafted chains start to elongate has no macroscopic signature.

Only the marginal regime has an effect on friction ($b \propto V$). In this regime, as was described in Section 2, the blob size of the elongated chains is equal to the entanglement blob size Λ_e, the force exerted on each grafted is constant (Eq. (6)) and the overall stress is given by:

$$\tau = \sigma\, \frac{kT}{\Lambda_e}\,. \tag{23}$$

Comparison of equations (22, 23) shows that the threshold velocity $V^\star$ for the onset of the marginal regime is proportional to the grafting density:

$$V^\star \propto \sigma. \tag{24}$$

The concept of saturated grafting has thus very important consequences. (i) The value of the extrapolation length (Eq. (21)), is independent of the grafting density. (ii) The extrapolation length dependence on velocity is monotonous: no sharp decrease is predicted. (iii) The threshold velocity $V^\star$ is proportional to the grafting density. All these predictions, which are independent of any model for the one-chain trapping number, must be compared to experimental results.

Experimental results

The recent results of the experiments by Durliat [14] provide interesting points of comparison with the models. The most interesting feature of his work is that a good control of the grafting density was achieved. The plateau value b_0

[15] No *quantitative* comparison can be drawn at this point, since this is still a one-chain model. Effects of the grafting density are addressed in the next section.

[16] In the framework of the tube renewal mechanism, the transition is described in different terms, see Section 6.

[17] In the 1992 total entanglement model and in the correlated binary entanglement number, the trapping number $X(V = 0) \propto N^{1/2}$ increases upon elongation, whereas it is constant ($X(V) \propto N$) in the binary entanglement model.

of the extrapolation length was found to be independent of grafting[18]:

$$b_0^{exp}(\sigma) = const. \tag{25}$$

And the threshold velocity $V^\star$ was found to be proportional to velocity:

$$V^\star_{exp} \propto \sigma \tag{26}$$

(except in the range of very high grafting densities, see Sect. 8).

These results can be considered as the signature of the saturated grafting regime (see Eqs. (21, 24)). The dependence of the extrapolation length b on the molecular weight P of the melt chains, is weak. The range is not wide enough, however, to be compared quantitatively with the power law of equation (21).

Hence, all experimental results indicate that the system is in the saturated grafting regime. There remains a strong discrepancy, however, concerning the absolute order of magnitude. In this regime, the extrapolation length should be of the order of the radius of gyration R_P of the melt chains, *i.e.*, about 50 nm. Measured values of b_0, however, are in the range of 1 to 3 μm. This discrepancy is yet unexplained. Possible origins are the numerical factors that were omitted in the whole theoretical study, as well as the perturbed conformations of the melt chains in the vicinity of the solid wall which might slightly influence entanglements.

At any rate, these results show that it was essential to take into account the influence of grafting, since the predictions are substantially altered in the saturated regime.

6 Specific improvements brought by the tube renewal approach

The tube renewal approach, described in Section 3, provides a new insight into the low velocity regime (low, constant $b = b_0$) and into the marginal regime ($b \propto V$). It also allows for a discussion of correlations between entanglements.

Low velocities

It was shown in Section 3 that for a number of reasons, the tube renewal mechanism is more realistic than the forced sliding mechanism at small V (for instance forced sliding cannot exist at low velocities, because chains escape by reptation).

The forced sliding and tube renewal friction mechanisms are valid when the melt chains are very mobile. It is also possible, however, that the grafted chain behave like a hard sphere, dragging all the fluid around it. The resulting "Stokes" friction can be written as $F_{Stokes} \simeq R_N \eta_P V$, by analogy with the drag of a solid sphere in a viscous fluid at low Reynolds numbers. The easier mechanism yields the real friction. Comparing this expression with equation (12), we find a natural threshold:

$$N^\star_K = \frac{N_e^2}{K^2} \tag{27}$$

where K is the tube renewal coefficient (Eq. (12)). The friction is given by the forced sliding or tube renewal mechanisms for $N \leq N^\star_K$, and by the Stokes formula for higher molecular weights. Using $K = 1$ as suggested by the discussion of correlations (see below), one recovers the results of the binary entanglement model (Eq. (14)) and the corresponding threshold (see discussion before Eq. (15)).

The regime of saturated grafting can also be interpreted in this context when $P > N$. Indeed, consider a melt chain whose center of gravity is roughly R_P away from the solid surface, so that it substantially interacts with the grafted layer (Fig. 5). The grafted chains appear as immobile obstacles. If they are sufficiently numerous, their effect on the melt chain is important. It cannot exceed, however, the effect of equivalent melt chains located below the surface level if it were in bulk[19] (Fig. 5b). In the equivalent bulk situation, those immobile chains are located at roughly R_P *below* the surface. The corresponding extrapolation length is thus of the order of $b \simeq R_P$. Hence, one recovers the result of the saturated grafting regime, (Eq. (21)) independently of any model [21].

When $P < N$, extinction of the melt velocity inside the brush occurs before the grafting density saturates [21], *i.e.*, the extrapolation length must be counted from the brush outer edge. The detailed brush conformation and concentration profile is then important. We do not develop this point.

Marginal regime

The constant friction force $F = kT/\Lambda_e$ in the marginal regime is due to the slight orientational bias of the stretched grafted chains. At low velocities ($V \leq V^{\star\star}$), lateral fluctuations of the grafted chains are limited by the tension that is transmitted along them. Above $V^{\star\star}$, lateral fluctuations are reduced because diffusion is slowed down. These features, which were developed in Section 3, are specific results of the tube renewal mechanism.

The velocity V_∞ that experimentally marks the end of the marginal regime received successive interpretations.

[18] In the linear regime described in the last sections (one-chain models), the extrapolation length was inversely proportional to the grafting density: $b \simeq (a^2 \eta_P V)/(\sigma F)$.

[19] Such a comparison between grafted chains and equivalent melt chains may seem rather far-fetched: in the equivalent bulk situation, an entanglement between two chains is released through the sliding of either chain, whereas in the real situation, the grafted chains have one end fixed and thus cannot slide out. In fact, the extra freedom in the equivalent bulk situation only reduces the efficiency of the entanglements by roughly a factor two. Hence, it does not alter the order of magnitude of the effect, and the comparison is thus relevant.

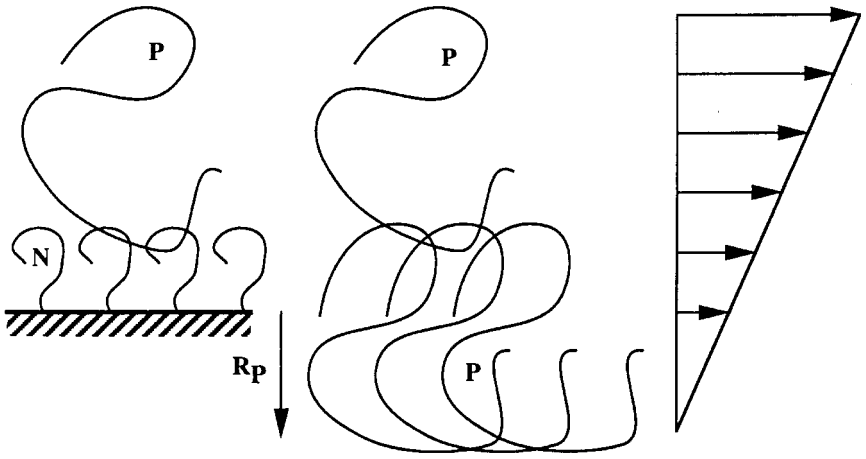

Fig. 5. Saturated grafting for $P > N$. Grafted chains (N) are present up to a distance R_N from the wall. If they are sufficiently densely grafted, they globally behave like P chains with their centres of gravity located at a distance R_P below the brush outer edge. The velocity profile then extrapolates to zero there. Hence, the smallest possible extrapolation length is of the order of the radius of gyration R_P of the melt chains.

In the 1992 model, it was interpreted as the crossover to Rouse friction (*i.e.*, $V_\infty = V_{Rouse}$). In reference [19], it was argued that the melt must behave like a quenched network at $V > V^{\star\star}$. The threshold V_∞ was therefore identified with $V^{\star\star}$. The tube renewal mechanism now shows that the friction $F \simeq F^\star$ is unchanged above $V^{\star\star}$. Thus, we go back to the initial interpretation: $V_\infty = V_{Rouse}$.

Correlations

It was shown in Section 3 that it was *a priori* possible to choose any value for the coefficient K of the tube renewal mechanism (Eq. (11)). In fact, choosing K so that it depends on N or on P amounts to introduce correlations between the local movements of a melt chain in different entanglement blobs along the grafted chain.

Indeed, the tube renewal friction force on a grafted chain (Eq. (12)) is equivalent to the following diffusion constant for the grafted chain:

$$D_K(N) = \frac{1}{X} D(N_e), \tag{28}$$

where X is the trapping number that corresponds to coefficient K (Eq. (14)) and where the constant k was omitted (Eq. (10)). Hence, X is the number of sub-objects that contribute to the diffusion of the whole chain independently. If we write:

$$X = \frac{1}{x}\frac{N}{N_e}, \tag{29}$$

the system behaves as if the N/N_e entanglement blobs Λ_e along the N chain were gathered into groups of $x = K^{-1}$ blobs each[20], such that the diffusion constant of each group is $D(N_e)$. Hence, each group behaves as if all x blobs were subjected simultaneously to the same fluctuation. Since fluctuations are due to the reptational motion of the melt chains, this means that melt chains act upon the x different blobs in the same direction, as if each melt chain had to pass on the same side of the grafted chain (*e.g.*, *always upstream from the N chain*) in the different entanglement blobs.

It seems highly unlikely that such correlations be present: although time correlations are clearly present (when one melt chain slides out, all corresponding constraints are released in quite a short time), spatial correlations such as those just described should not be present (except at velocities close to $V^{\star\star}$).

In Section 4, we presented models of the trapping number X in which the corresponding parameter K is non-constant: $K = N_e/N^{1/2}$ in the total entanglement model, $K = N_e^{1/2}/N^{1/2}$ in the correlated binary entanglement model. This feature alone might be sufficient to rule out these models. The above argument concerning the absence of correlations, however, does not take into account the possible influence of stress fluctuations in the melt, due to reptation (see Ref. [29] and the comments in [21], see also Ref. [30]). Hence, further arguments or experimental tests will be needed for further progress on this point, although the present approach, based on the initial reptation theory, rules out all models except the binary entanglement model ($K = 1$ and $X = N/N_e$)[21].

7 Choice of a model?

It was shown in Section 5 that the experimental situation [14] corresponds to the saturated grafting regime (Eq. (26)). In this regime, the overal friction of the grafted layer is independent of the detailed friction of one chain if it were alone: it does not depend on the model chosen for the trapping number X (forced sliding mechanism) or equivalently for the tube renewal coefficient K (see Eq. (14)).

Hence, the models cannot be tested in this way. This issue is important, however, since each model is based on some assumption concerning the entanglements (total,

[20] Whether these x blobs are spatially close to one another or not does not matter.

[21] The above arguments in fact imply $K = k$. But further arguments show that $K = 1$ (see Sect. 7 and Eq. (32)).

binary or correlated binary entanglements for instance). These assumptions concerning interfacial entanglements (between a grafted, fixed chain, and moving, melt chains) can be compared to the models that were developed to predict the value of the entanglement mass of a polymer from its molecular parameters (persistence length, chain contour concentration[22]).

Different models

Discussing correlations in the tube renewal approach shows that in fact only the binary entanglement model ($K = 1$ or $X = N/N_e$) should be correct (Sect. 6). But as was pointed out, this discussion is not sufficient because the tube renewal approach itself is based on reptation and includes the corresponding limitations (viscosity scales like P^3 instead of $P^{3.4}$). Hence, further arguments are required to choose between the models.

	$P < N$		$P > N$	
Model	K	X	K	X
Binary	1	N/N_e	1	N/N_e
Corr. Bin.	$N_e^{1/2}/P^{1/2}$	$N/(P^{1/2}N_e^{1/2})$	$N_e^{1/2}/N^{1/2}$	$N^{1/2}/N_e^{1/2}$
Total	$N_e/P^{1/2}$	$N/P^{1/2}$	$N_e/N^{1/2}$	$N^{1/2}$
Klein	$1/P^{1/2}$	$N/(P^{1/2}N_e)$		
Monfort *et al.*	N_e^2/P	$N/(P^{0.6}N_e)$		

Apart from the three models presented in Section 4 (total, binary and correlated binary entanglement models), existing models for friction are the model by Klein [33] and the model by Montfort, Marin and Monge [34]. Both are based on the tube renewal approach, but as they were developed for a bulk situation, they only deal with the situation of a long test chain N immersed in a melt of shorter molecules, $P < N$: the reptation of the long test chain N is slow and thus the tube renewal due to reptation of the melt chains is relevant for the diffusion of the test chain.

The values of the trapping number X and of the tube renewal coefficient K in all these models are given above.

In the following paragraphs, arguments are taken from comparison with the well-known disentangled friction regime and a suggestion is presented for a possible comparison with experiments.

Consistence with non-entangled friction

At $P \simeq N_e$, the friction between the grafted chain N and the melt evolves from a non-entangled situation ($P < N_e$) to an entangled mechanism ($P > N_e$). At the transition, friction is expected to display a smooth crossover. Indeed, this transition is very similar to the bulk viscosity transition between non-entangled and entangled melt: although the dependence on the molecular weight P is changed at the transition (from P to $P^{3.4}$), no discontinuity appears[23].

Friction in the non-entangled regime ($P < N_e$) is known to be linear in N for short grafted chains: $F = N\zeta_0 V$. It is also known to be equivalent to the Stokes friction on a hard sphere for an athermal solvent ($P \simeq 1$): $F \simeq aN^{3/5}\eta_0 V$. In the intermediate situations ($P \geq 1$), friction can be obtained [17] as the result of the competition between the Stokes, hard sphere friction in the melt (viscosity proportional to P) and the Rouse friction. The resulting expression for friction is given by[24]:

$$F \simeq aN^{3/5}P^{-1/5}\ P\eta_0 V \qquad (P \leq N^{1/2}) \qquad (30)$$

$$F \simeq N\zeta_0 V \qquad (P \geq N^{1/2}). \qquad (31)$$

The above expressions for unentangled friction and the expressions for the entangled regime provided by the models ($N \geq N_e$ and $P \geq N_e$) coincide at the transition $P \simeq N_e$ if the tube renewal coefficient K is unity at the transition. The corresponding form of K and X above the transition are proportional to some power of P/N_e:

$$K = \left(\frac{P}{N_e}\right)^{\beta}$$

$$X = \frac{N}{N_e}\left(\frac{P}{N_e}\right)^{\beta} \qquad (P \geq N_e). \qquad (32)$$

Comparison of this condition with the expressions from all models leads to rule out the total entanglement model and the models by Montfort *et al.* and by Klein: only the binary and the correlated binary entanglement models are compatible with this continuity condition. Any further choice will require experimental tests.

A possible experimental test

In the case of short melt chains ($P \leq N$), the binary and the correlated binary entanglement models yield predictions that have the same dependence on N: they differ by a power of the melt chain length P. A comparison with experiment on this basis would be rather non-conclusive because P-dependences are not very well understood (P^3 *versus* $P^{3.4}$ problem).

A difference between the models, concerning the N-dependences, can be found in the $P \geq N$ regime (long melt chains). This regime has been studied in the slippage experiments [14]. But the low grafting densities that were achieved are still not low enough to avoid grafting saturation (see Sect. 5). Hence, these experiments do not provide a test between these models yet.

[22] For a detailed discussion, see the generic model by Graessley and Edwards [31] and a review of the specific models by Colby, Rubinstein and Viovy [32]. Additional remarks can be found in [21].

[23] Conversely, at the corresponding transition for the grafted chain in an entangled melt ($P > N_e$ and $N \approx N_e$), important variations of the friction would be expected, since the relaxation of a grafted chain in an entangled medium is very much slower than that of a shorter chain: the relaxation time is known to increase exponentially with the chain length [24].

[24] For a derivation of this result in terms of a perturbation of the velocity field, see [21].

Since such low grafting densities are very difficult to obtain at an interface, a similar situation in bulk has to be found. But in bulk, if the test chain N is shorter than the melt chains, then its own reptational motion is the fastest relaxation process, and thus the tube renewal mechanism cannot be observed. The only way out of this is to lock reptation. This can be done by using a branched molecule [24].

For instance, let us consider a star polymer made of three or four arms (N monomers each). The usual reptation motion of a linear molecule is locked. Hence, diffusion of the molecule will occur mainly through two mechanisms: the Stokes hard sphere mechanism and the tube renewal mechanism. For a melt of long P molecules, the relevant mechanism is tube renewal, and the diffusion of the test molecule reflects the details of this mechanism, *i.e.*, the model: for such a small number of arms, no grafting saturation is present and the diffusion constant is immediately deduced from the expression for friction given by the models.

A test between the remaining models (and all other possible models that satisfy Eq. (32)) can thus be provided by a study of the diffusion constant of star polymers in a melt of longer, linear molecules. It is necessary to vary the arm length and to record the corresponding variations of the diffusion constant. Precise synthesis of stars is thus required. Laser velocimetry and photobleaching techniques should then provide a mean for measuring the corresponding very slow diffusion dynamics.

To summarize, no final test of the models for the trapping number has been carried out yet. Two models are still valid: the binary entanglement model and the correlated binary entanglement model.

8 Very high grafting densities: a new topological behaviour?

In the saturated grafting regime as it was described in Section 4, the threshold velocity $V^\star$ for the onset of the marginal regime is found to be proportional to the grafting density σ (Eqs. (24, 26)). Below $V^\star(\sigma)$, chains are progressively stretched as the velocity is increased. It was also shown (Sect. 3) that grafted chains are stretched ($\Lambda \simeq \Lambda_e$) and flushed against the solid wall when $V \geq V^{\star\star}$.

Therefore, at very high grafting densities, when it is expected that $V^\star(\sigma) > V^{\star\star}$, the above descriptions yield contradictory predictions for the conformations of the grafted chains for $V^{\star\star} \leq V \leq V^\star(\sigma)$: on the one hand, they should be only partially stretched since they should not have reached the marginal regime ($V \leq V^\star(\sigma)$), and on the other hand, they should be marginally stretched (blob size Λ_e) and flushed against the wall ($V \geq V^{\star\star}$). We therefore expect a sudden elongation of the chains at some velocity $V^\star_{\mathit{eff}}(\sigma) \leq V^{\star\star}$.

Hence, at grafting densities higher than

$$\sigma^{\star\star} \simeq \frac{a\eta_P\,\Lambda_e^2}{kT\,T_{rep}(P)}\sigma_{Pmax}, \qquad (33)$$

although the exact mechanism for it is not understood, we expect a drop in $b(V)$ at some velocity $V^\star_{\mathit{eff}}(\sigma) \leq V^{\star\star}$. Experimentally, a decrease of $V^\star(\sigma)$ is indeed observed beyond some threshold grafting density. Furthermore, some of the data presented by Durliat [14] for high grafting densities do not seem to be incompatible with a drop of $b(V)$.

The precise behaviour of the grafted chains in such a regime is not understood yet. We suspect the existence of a new topological behaviour, however. Indeed, stretched chains are fixed at one point, oriented along the direction of flow and mutually entangled laterally. Thus, they have a "braid" geometry: the corresponding results from the theory of knots (see for instance Ref. [35]) should be partly applicable. Here, grafted chains are combed by the flow of the entangled melt and conversely, lateral fluctuations of the chains ensure reentanglement. Upon increasing the melt velocity, the braid is progressively disentangled. A more detailed work on this point will be required.

9 Conclusions

We discussed different molecular models for wall slip of polymer melts. The 1992 model, whose predictions display a marked qualitative discrepancy with experimental results, is a one-chain model based on the total entanglement assumption; friction is described through the forced sliding mechanism. We showed that the tube renewal mechanism is more realistic a description of friction, and that it predicts new features of the marginal regime (Sects. 3, 6). Different assumptions can be made concerning entanglements: binary model, correlated binary model (Sect. 4). But these models yield different predictions only if the grafting density is very weak (Sect. 5). Such weak grafting densities have not been obtained experimentally yet. But it was indicated (Sect. 7) that some models can be ruled out because they do not crossover to the correct disentangled friction as melts of shorter molecules are used, and that a study of the diffusion dynamics of star polymers in a melt of longer chains could provide a test between the remaining models. The determination of the correct model should yield an interesting point of view on the nature of entanglements (see beginning of Sect. 7).

Two main directions for future theoretical work were outlined. It was shown (Sect. 8) that at very high grafting densities, topological effects due to the mutual entanglements of the grafted chains are expected to arise. In the practical situation of an adsorbed polymer layer, the volume fraction of the layer is not negligible, mutual entanglements exist and similar effects should be present, with some differences due to the fact that adsorbed chains contain mainly loops, rather than tails.

Another direction is the network limit (with a melt of ultra-long chains). The rearrangement of grafted chains then becomes the dominant relaxation process: grafted chains retract and relax back into the melt. This mechanism is similar to the "reptation" of branched polymers.

I am very grateful to F. Boué, P. Fabre, P.-G. de Gennes, L. Leibler and E. Raphaël for very interesting discussions, and

to F. Boué for suggesting a test of the predictions concerning transverse fluctuations of the grafted chains. I wish to thank the team of the Laboratoire CNRS-Elf Atochem where the present text was completed.

References

1. M. Mooney, J. Rheol. **2**, 1931.
2. P.-G. de Gennes, C. R. Acad. Sci. **288 B**, 219 (1979).
3. J.J. Benbow, P. Lamb, SPE Trans. **3**, 1963.
4. A.V. Ramamurthy, J. Rheol. **30**, 337 (1986).
5. N. El Kissi, J.M. Piau, J. Non-Newtonian Fluid Mech. **37**, 55 (1990).
6. S.G. Hatziriakos, J.M. Dealy, J. Rheol. **36**, 845 (1992).
7. Y. Inn, S.Q. Wang, Phys. Rev. Lett. **763**, 467 (1996).
8. M.M. Denn, Annu. Rev. Fluid Mech. **22**, 13 (1990).
9. K. Migler, H. Hervet, L. Leger, Phys. Rev. Lett. **703**, 287 (1993).
10. L. Leger, H. Hervet, G. Massey, E. Durliat, J. Phys.-Cond. **9**, 7719 (1997).
11. N. El Kissi, L. Leger, J.M. Piau, A. Mezghani, J. Non-Newtonian Fluid Mech. **52**, 249 (1994).
12. L. Leger, H. Hervet, Y. Marciano, M. Deruelle, G. Massey, Israel J. Chem. **35**, 65 (1995).
13. E. Durliat, H. Hervet, L. Leger, Europhys. Lett. **38**, 383 (1997).
14. E. Durliat, Ph.D. thesis, University of Paris-6, 1997.
15. F. Brochard-Wyart, P.-G. de Gennes, Langmuir **8**, 3033 (1992).
16. A. Ajdari, F. Brochard-Wyart, P.-G. de Gennes, L. Leibler, J.-L. Viovy, M. Rubinstein, Physica A **204**, 17 (1994).
17. F. Brochard-Wyart, A. Ajdari, L. Leibler, M. Rubinstein, J.-L. Viovy, Macromol. **27**, 803 (1994).
18. A. Ajdari, F. Brochard-Wyart, C. Gay, P.-G. de Gennes, J.-L. Viovy, J. Phys. II France **5**, 491 (1995).
19. F. Brochard-Wyart, C. Gay, P.-G. de Gennes, Macromol. **29**, 377 (1996).
20. C. Gay, J. Phys. II France **6**, 335 (1996).
21. C. Gay, Ph.D. thesis, University of Paris-6, 1997.
22. F. Brochard-Wyart, P.-G. de Gennes, P.A. Pincus, C. R. Acad. Sci. **314 II**, 873 (1992).
23. P.-G. de Gennes, MRS Bulletin **16**, 20 (1991).
24. P.-G. de Gennes, J. Phys. France **36**, 1199 (1975).
25. P.-G. de Gennes, Scaling Concepts in Polymer Physics, (Cornell Univ. Press, Ithaca, 1979).
26. P.A. Pincus, Macromol. **9**, 386 (1976).
27. J. Klein, Nature **271**, 143 (1978).
28. M. Daoud, P.-G. de Gennes, J. Polym. Sci. **17**, 1971 (1979).
29. M. Rubinstein, S.P. Obukhov, Phys. Rev. Lett. **71**, 1856 (1993).
30. A.N. Semenov, M. Rubinstein, Eur. Phys. J. B **1**, 87 (1998).
31. W.W. Graessley, S.F. Edwards, Polymer **22**, 1329 (1981).
32. R.H. Colby, M. Rubinstein, J.-L. Viovy, Macromol. **25**, 996 (1992).
33. J. Klein, Macromol. **19**, 105 (1986).
34. J.P. Monfort, G. Marin, P. Monge, Macromol. **17**, 1551 (1984).
35. P. Dehornoy, Pour la Science, avril, 68 (1997).